CRYSTAL GROWTH & DESIGN

Open Access
This article is licensed under CC-BY 4.0

pubs.acs.org/crystal
Article

Structural Diversity in Copper(II) Complexes with NNO Tridentate Schiff Bases and Chlorido Ligands: The Realm of N−H···O and N−H···Cl Hydrogen Bonds and Their Steric and Electronic Modulations

Matteo Mari, Stefano Baratti, Chiara Canovi, Anita Ballerini, Francesco Genua, Kevin D'Addazio, Samuele Pellacani, Alessio Nicolini, Lara Gigli, Maurizio Polentarutti, Simone d'Agostino, Dominga Rogolino, Mauro Carcelli, and Luca Rigamonti*

Cite This: *Cryst. Growth Des.* 2026, 26, 9073−9084

Read Online

ACCESS | Metrics & More | Article Recommendations | Supporting Information

ABSTRACT: In this paper, we investigated the N−H···O and N−H···Cl hydrogen bonds (H-bonds) in determining the crystal packing in copper(II) complexes with NNO tridentate Schiff bases and chlorido ligands of general formula [Cu(^{G}Ln^{R1,R2})(Cl)]. The ligands derive from the monocondensation of G-substituted salicylaldehydes with modulated electronic character (G-salH, G = NO_2, H, and OMe) and aliphatic diamines with either variable length or steric hindrance of the chain (Ln: L1 = ethylene bridge, en; L2 = propylene bridge, tn; and L3 = 2,2-dimethylpropylene bridge, Me_2tn) and different degrees of alkylation of the coordinated amino group (R1, R2 = H and Me). Structural data from both single crystal and powder X-ray diffraction studies were successfully obtained for nearly all synthesized compounds, and they all crystallize with no solvent molecules, allowing the study of the H-bonds among [Cu(^{G}Ln^{R1,R2})(Cl)] units without solvent interference. The synergism among the different steric and electronic factors, together with the tendency of copper(II) to modulate its coordination environment from square planar to square pyramidal or trigonal bipyramidal with the addition of a fifth position, reveals an intriguing structural diversity, which can also be envisaged with the help of multivariate analysis.

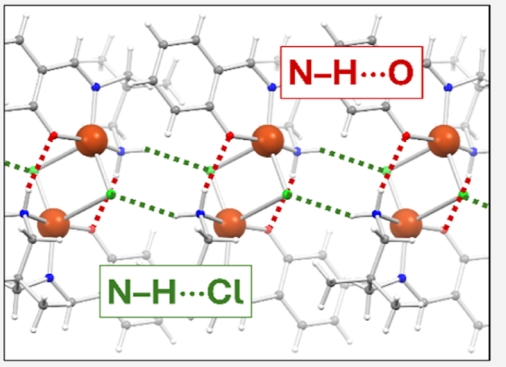

INTRODUCTION

The fundamental role of hydrogen bonds (H-bonds)[1] in determining the crystal packing of molecular materials is indisputable,[2] and the study of their nature and strength[3,4] is of crucial interest in rationalizing the intermolecular interactions driving solid-state structures.[5]

Over the past few years, our research has been focused on copper(II) complexes with NNO tridentate Schiff base ligands derived from G-substituted salicylaldehydes (G-salH) and aliphatic primary diamines such as ethane-1,2-diamine (en) and propane-1,3-diamine (tn). The template synthetic routes to avoid double condensation on both primary amino groups have been deeply explored,[6] leading to mono-, di-, and tri-nuclear compounds depending on the reaction conditions.[7] The structural characterization of these derivatives has always played a central role, especially when magnetic properties represented the focus.[7−9] The presence of the coordinated primary amino group allowed the employment of such compounds as useful synthons for unsymmetrically substituted push−pull salen/saltn derivatives, which are interesting for their non-linear optical properties either in solution[10] or in the solid state.[11] Furthermore, the lability of the fourth coordinated ligand, such as pyridine in mononuclear compounds or bridging phenoxido oxygen atoms in dinuclear species, allows the conversion into new species,[8] as we recently performed with the insertion of the chlorido anion as fourth ligand and the study of the cytotoxic properties of the so-obtained complexes.[12,13]

These latter compounds[12,13] show intriguing structural peculiarities in the solid state, like the formation of polymeric chains or dimeric units among [Cu(L)Cl] units involving N−H···O or N−H···Cl H-bonds. Moreover, a certain degree of variability of the displacement of the chlorido ligand from the NNOCu coordination plane was observed, a fact that modulates the dimeric geometry. The diamines employed so far were en[12] and tn,[13] while G was 5-NO_2, H, or 5-OMe.

As further study, we have then decided to expand the family of copper(II) complexes of general formula [Cu(^{G}Ln^{R1,R2})(Cl)] (**A1**−**A9**, **B1**−**B6**, and **C1**−**C6**, Table 1) with the aim of investigating the N−H···O and N−H···Cl H-bonds in the solid state. The NNO tridentate Schiff base ligands (^{G}Ln^{R1,R2})$^{-}$

Received: September 4, 2026
Revised: October 7, 2026
Accepted: October 8, 2026
Published: October 16, 2026



ACS Publications
© 2026 The Authors. Published by American Chemical Society

https://doi.org/10.1021/acs.cgd.6c01323
Cryst. Growth Des. 2026, 26, 9073−9084

Downloaded from pubs.acs.org/cgdefu/article-pdf/26/21/9073/6892110/cg6c01323.pdf by UNIV DEGLI STUDI DI MODENA user on 06 November 2026

Table 1. Scheme of Copper(II) Complexes Here Studied and Relevant Crystal Packing Features of $[Cu(^{G}Ln^{R1,R2})(Cl)]$ Units[15,16]

Molecular scheme	Compound	G	R1, R2	X-ray data	Space group	Main crystal packing features
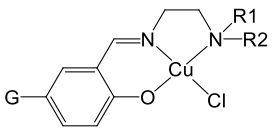 $[Cu(^{G}L1^{R1,R2})(Cl)]$	**A1** [12]	NO_2	H, H	1993219 – VUJFOY	orthorhombic $Pna2_1$	polymeric 1D chain via Cl and N–H···O
	A2 [12]	H	H, H	1966426 – HAJTOD02 (100 K) [12] 794469 – HAJTOD (293 K) [15]	monoclinic $P2_1/c$	dimeric unit via Cl and N–H···O
	A3 [12]	OMe	H, H	1966425 – VUJFAK	monoclinic $P2_1/c$	dimeric unit via Cl and N–H···O
	B1	NO_2	H, Me	this work – 2551462	orthorhombic $Pca2_1$	pseudo zig-zag 1D chain via Cl and N–H···O
	B2	H	H, Me	this work – 2551458 (100 K) 2214190 – BEYKAV (180 K) [16]	orthorhombic $P2_12_12_1$	pseudo zig-zag 1D chain via Cl and N–H···O
	B3	OMe	H, Me	this work – 2551459 **B3-I** this work – 2551460 **B3-II**	monoclinic $P2_1/c$ (**B3-I**) *Pbca*(**B3-II**)	pseudo zig-zag 1D chain via Cl and N–H···O dinuclear unit via O and Cl
	C1	NO_2	Me, Me	this work – 2551453	monoclinic $P2_1/c$	pseudo zig-zag 1D chain via Cl
	C2	H	Me, Me	this work – 2551454 this work – 2551457 $(\mathbf{C2})_2CuCl_2$	orthorhombic *Pbca*	pseudo zig-zag 1D chain via Cl
	C3	OMe	Me, Me	this work – 2551456	orthorhombic *Pbca*	pseudo zig-zag 1D chain via Cl
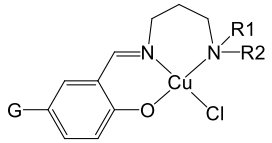 $[Cu(^{G}L2^{R1,R2})(Cl)]$	**A4** [13]	NO_2	H, H	no X-ray data	–	–
	A5 [13]	H	H, H	2424407 – IKEKOC	monoclinic $P2_1/c$	dimeric unit via Cl and N–H···O
	A6 [13]	OMe	H, H	2423929 – IKEKIW	monoclinic $P2_1/c$	dimeric unit via Cl and N–H···O
	B4	NO_2	H, Me	this work – 2551463	monoclinic $P2_1/c$	polymeric 1D chain via Cl and O
	B5	H	H, Me	this work – 2551461 **B5**_SCXRD this work – 2551464 **B5**_PXRD	orthorhombic $P2_12_12_1$	pseudo zig-zag 1D chain via Cl
	B6	OMe	H, Me	no X-ray data	–	–
	C4	NO_2	Me, Me	this work – 2560838	monoclinic $P2_1/n$	dimeric unit via Cl
	C5	H	Me, Me	this work – 2560839	monoclinic $P2_1/n$	dinuclear unit via O
	C6	OMe	Me, Me	this work – 2560840	triclinic $P\bar{1}$	dinuclear unit via O
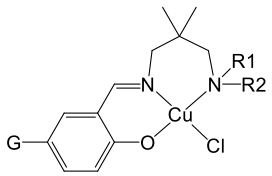 $[Cu(^{G}L3^{R1,R2})(Cl)]$	**A7**	NO_2	H, H	no X-ray data for **A7** this work – 2551469 **M7**	–	–
	A8	H	H, H	this work – 2551397 **A8** this work – 2551401 **D8'** this work – 2551452 **D8"**	monoclinic $P2_1/c$	dimeric unit via Cl and N–H···O
	A9	OMe	H, H	this work – 2560841	monoclinic $P2_1/n$	dimeric unit via Cl and N–H···O

derive from the monocondensation of G-salH with a modulated electronic character (G-salH, G = 5-NO_2, H, and 5-OMe) and aliphatic diamines with either variable length or steric hindrance of the chain (Ln: L1 = ethylene bridge, en; L2 = propylene bridge, tn; and L3 = 2,2-dimethylpropylene bridge, Me_2tn). In addition, different degrees of alkylation of the coordinated amino group (R1, R2 = H, Me) were introduced (see Table 1 for molecular schemes, nomenclature, and details on substituents G and the diamine employed). The structural data from both single crystal (SCXRD) and powder (PXRD) X-ray diffraction studies could be retrieved on almost all the synthesized compounds, and they all do crystallize with no solvent molecules, a fact that ensures the study of the H-bonds among $[Cu(^{G}Ln^{R1,R2})(Cl)]$ units with no interference.

Together with the new derivatives here synthesized and structurally characterized, we searched for homologous copper(II) compounds with an NNOCl square planar coordination in the Cambridge Structural Database (CSD) (see Table S1 in Supporting Information). Their structural features were then implemented into a multivariate analysis through principal component analysis (PCA)[14] with the aim of rationalizing the balance among the coordination needs of copper(II) and the intermolecular interactions through N–H···O, N–H···Cl, and other contacts in determining the crystal packing.

RESULTS AND DISCUSSION

Synthetic Procedures

Compounds **A1**–**A9**, invariantly from the use of the primary diamine en (L1), tn (L2), or Me_2tn (L3), present only one imino group derived from the condensation of one of the amino groups with the substituted G-salH, while the second amino group of the diamine is retained and coordinates the copper(II) center. Note that a template synthetic strategy is here required to avoid double condensation.[6] We already reported on the synthesis of **A1**–**A3**[12] and **A4**–**A6**,[13] which could be obtained starting from the mononuclear $[Cu(^{G}Ln^{H,H})(py)](ClO_4)$ (n = 1 and G = 5-NO_2 (**M1**), H (**M2**); n = 2 and G = 5-NO_2 (**M4**), H (**M5**))[7,17] or the dinuclear $[Cu_2(\mu\text{-}^{G}Ln^{H,H})_2](ClO_4)_2$ (n = 1

Downloaded from pubs.acs.org/cgdefu/article-pdf/26/21/9073/6889211/0/cg6c01323.pdf by UNIV DEGLI STUDI DI MODENA user on 06 November 2026

https://doi.org/10.1021/acs.cgd.6c01323
Cryst. Growth Des. 2026, 26, 9073–9084

Scheme 1. Schematic Representation of the Synthesis of Complexes A and Byproducts D5′ and D8′ (Diamine Bridge is Shown as ∩)

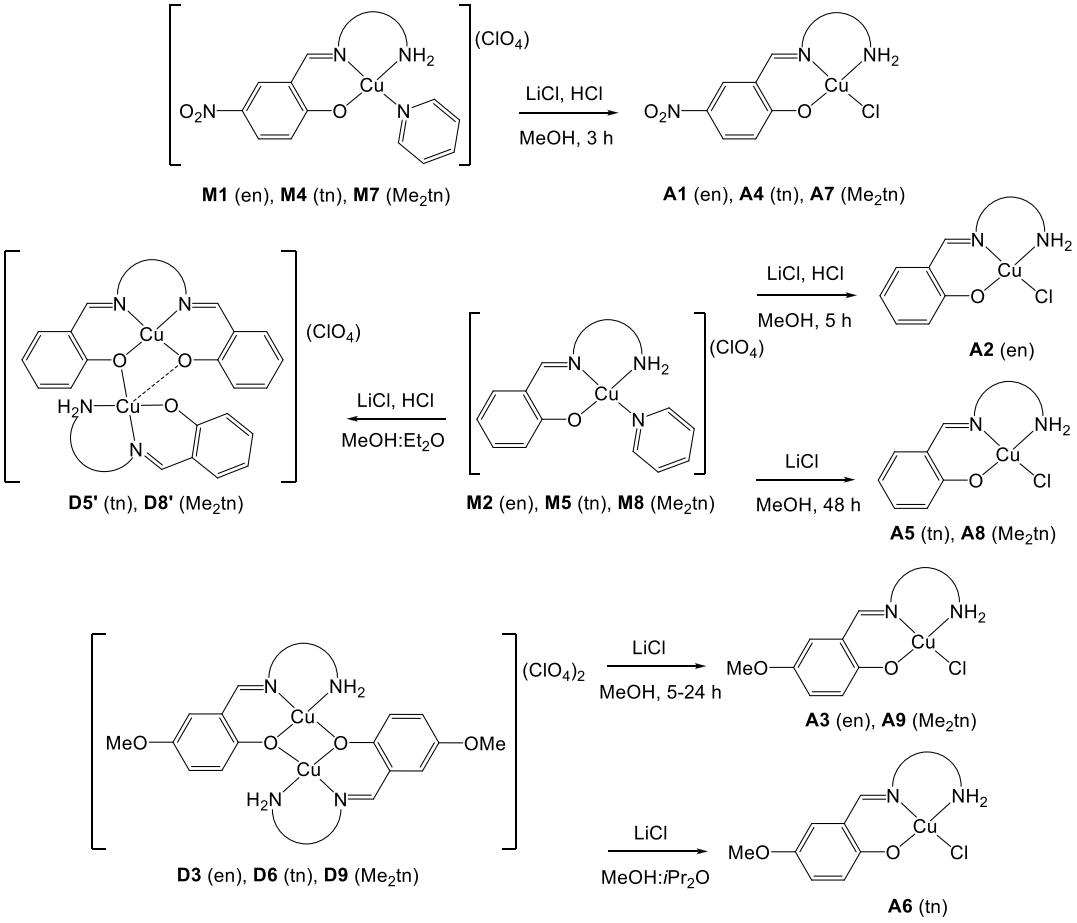

and G = H (**D2**), 5-OMe (**D3**); n = 2 and G = H (**D5**), 5-Ome (**D6**))[7,18] employed as precursors (Scheme 1).

In this work, we expanded the template method to obtain the mononuclear complexes $[Cu(^{G}L3^{H,H})(py)](ClO_4)$ (G = 5-NO_2 (**M7**), H (**M8**)) and the dinuclear complex $[Cu_2(\mu\text{-}^{5-OMe}L3^{H,H})_2](ClO_4)_2$ (**D9**) with the employment of Me_2tn (see Scheme 1), applying synthetic procedures similar to the ones previously reported.[7] These precursors were then reacted with lithium chloride in MeOH either in the presence of HCl or without the addition of acid, depending on the starting precursor (see Experimental Section in Supporting Information for further details), yielding the desired products **A7**−**A9**. In particular, as for tn derivatives,[13] the presence of the nitro group confers sufficient stability to allow the employment of aqueous HCl to promote the expulsion of pyridine from **M7** and coordination of chlorido anion to obtain **A7** within 3 h at about 25 °C. The yield is about 83% thanks to the low solubility granted by the nitro group. Considering also the synthesis of **M7** with a yield of about 50% starting from commercial reagents, the overall yield of **A7** was approximately 42%.

In the case of **A8** (G = H), the optimal reaction conditions involve longer reaction times (48 h) in the presence of an excess of LiCl, avoiding the addition of HCl as for **A5**,[13] with a moderate yield of 36%, which lowers to 20% as the overall yield also considering the synthesis of its precursor **M8**. When employing only LiCl, crystals of **A8** formed upon crystallization of the methanol reaction mixture. On the other hand, the presence of HCl led to the crystallization of the byproduct $[Cu_2(\mu\text{-salMe}_2tn)(^{H}L3^{H,H})(MeOH)](ClO_4)$ (**D8′**), which also contaminates the bulk solid isolated from the reaction, in analogy to what was observed in the synthesis of **A5** and the formation of **D5′** (Scheme 1).[13] This dinuclear species is evidently the result of a rearrangement in solution where salMe$_2$tn (*N*,*N*′-bis(-salicylidene)-2,2-dimethyl-1,3-diaminopropane) results from double condensation. This rearrangement in solution could also be observed upon crystallization of the reaction mixture of **M8**, where crystals of the dinuclear species $[Cu_2(\mu\text{-salMe}_2tn)(py)_2](ClO_4)_2$ (**D8″**) separate out (see Supporting Information for structure description of **M7**, **D8′**, and **D8″**).

The reaction of **D9** with LiCl in a two-fold excess at about 25 °C, followed by slow evaporation of the solvent for 10 days, led to the desired product **A9**, in line with what was observed with **A3**[12] but in contrast with **A6**.[13] The conversion is undoubtedly confirmed upon infrared (IR) inspection since the disappearance of the perchlorate stretching signals around 1100 cm^{-1} and the shift of the N−H stretching bands with respect to the precursor are strongly diagnostic of the occurred reaction.

A different strategy was used for the synthesis of **B1**−**B3**, **B4**−**B6**, **C1**−**C3**, and **C4**−**C6** deriving from diamine enMe, tnMe (R1 = H, R2 = Me), enMe$_2$, and tnMe$_2$ (R1 = R2 = Me). Unlike type **A** complexes, the presence of only one primary amino group simplifies the synthetic route, which therefore does not require the application of a template method. The direct reaction between the aldehyde and the diamine to generate the tridentate Schiff base $H^{G}L1^{H,Me}$, $H^{G}L2^{H,Me}$, $H^{G}L1^{Me,Me}$, and $H^{G}L2^{Me,Me}$ *in situ* in solution, and subsequent reaction with

Downloaded from pubs.acs.org/cgdefu/article-pdf/26/21/9073/6889210/cg6c01323.pdf by UNIV DEGLI STUDI DI MODENA user on 06 November 2026

https://doi.org/10.1021/acs.cgd.6c01323
Cryst. Growth Des. 2026, 26, 9073−9084

Scheme 2. Schematic Representation of the Synthesis of Complexes B and C (Diamine Bridge is Shown as ∩)

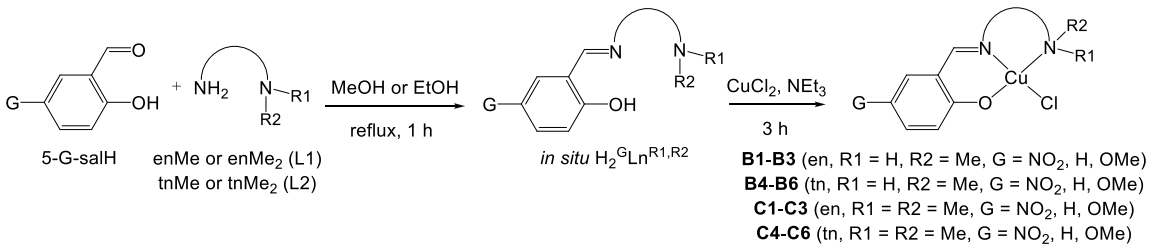

copper(II) chloride can be conducted in MeOH or EtOH using 5-G-salH (G = 5-NO_2, H, and 5-OMe) and enMe/tnMe/enMe$_2$/tnMe$_2$ under reflux for 1 h. During the reaction, triethylamine (NEt_3) was used to deprotonate the phenolic group, and after that $CuCl_2 \cdot 2H_2O$ was added, either as a water solution or solid (Scheme 2).

For **B5** and **B6**, EtOH was the solvent of choice, while for all the other complexes of the **B** series, MeOH was employed. In fact, **B5** and **B6** proved to be highly soluble in MeOH, a fact that limits the formation of a precipitate, probably aided by the water used to solubilize the copper(II) chloride. Replacing MeOH with EtOH and excluding water proved to be the correct choices for optimizing the synthesis and obtaining **B5** and **B6** as microcrystalline powder solids directly from the mother liquor.

Following the method reported above, **C2** does not crystallize during the reaction in either EtOH or MeOH. Therefore, its synthesis was conducted in MeOH or EtOH, without the addition of water to dissolve the copper(II) chloride and then adding a two-fold excess of Et_2O (the addition of *n*-hexane instead of Et_2O led to similar results when EtOH was employed). The resulting mixtures finally led to the formation of the desired product as deep-green crystals after refrigeration. To improve metal coordination, the copper(II) salt was used in excess in a synthetic attempt, leading instead to the formation of **(C2)$_2$CuCl$_2$** as a product after crystallization with Et_2O. In this trinuclear species, two $[Cu(^{H}L1^{Me,Me})(Cl)]$ moieties are bridged by a $CuCl_2$ unit (see Supporting Information for structure description).

Similarly, the synthesis of **C4**−**C6** was conducted in EtOH by using solid $CuCl_2 \cdot 2H_2O$ with no water addition. After reflux, **C4** directly precipitates from the reaction mixture upon cooling to about 25 °C, while **C5** crystallizes overnight at 4 °C without any co-precipitating solvent. **C6**, instead, requires the addition of an excess of Et_2O and 48 h at 4 °C to allow crystallization.

Elemental analysis and mass spectrometry confirmed the nature of all the compounds obtained, together with IR spectroscopy as a diagnostic technique, in particular for C═N bond formation and the presence or absence of N−H stretching bands.

X-ray Crystal Structure Characterization

Single crystals suitable for SCXRD experiments were obtained upon cooling of the reaction mixture for **B2**, slow evaporation of the methanolic reaction mixture for **B3-II** and **D8′**, slow diffusion of Et_2O into the methanol reaction mixture for **B2**, **B3-I**, **C1**, **C2**, **C3**, **(C2)$_2$CuCl$_2$**, **B5**, **A8**, and **D8″**, slow diffusion of $^{i}Pr_2O$ into the methanol reaction mixture for **B5**, slow diffusion of a EtOH:$^{i}Pr_2O$ 1:1 mixture into a DMSO solution for **A9**, slow diffusion of ^{i}PrOH into a DMSO solution for **C4**, slow diffusion of *n*-hexane into a ^{i}PrOH solution for **C6**, and slow diffusion of *n*-hexane into a THF/EtOH 1:1 solution for **C5**. Single crystal data and details of data collection are summarized in Table S2 in Supporting Information, where only the best data are reported for **B2** and **B5**. Samples of **B1**, **B4**, **B5**, and **M7** were instead suitable for PXRD, and structure determination was obtained from collected data. Powder crystal data and details of data collection are summarized in Table S3 in Supporting Information. The Rietveld refinement was carried out using TOPAS Academic V5[19], in which soft restraints on atomic distances (±0.03 Å) and angles (±0.1°) were applied. The Rietveld refinement profile fits of the experimental powder diffraction patterns, obtained after the simulated annealing of the model with EXPO14,[20] are reported in Figure S1 in Supporting Information. Table 1 reports the space groups of all derivatives and the main crystal packing features, which are described and compared in details in the following together with the available literature data for **A1**, **A2**, **A3**, **A5**, and **A6**.[12,13]

Table 2. Structural Features of the Fifth Cu···Cl Apical Interactions[ab]

	Cu···Cl (Å)	Cu-Cl···Cu (°)	Cl−Cu···Cl (°)
A1[a]	2.672	99.9	100.4
A2	2.781(1)	77.90(1)	102.10(1)
A3	2.784(1)	78.46(2)	101.54(2)
A5	2.6984(6)	83.152(13)	96.847(13)
A6	2.8430(5)	81.29(2)	98.71(2)
A8	2.850(1)	81.25(4)	98.75(4)
A9	2.8929(9)	81.57(3)	98.43(3)
B1	3.265(1)	80.72(2)	109.36(3)
B2	2.940(2)	89.76(6)	107.82(7)
B3-I	3.116(2)	92.63(5)	109.74(5)
B5[b]	2.7106(6)	101.13(1)	122.10(1)
C1	2.710(1)	136.68	98.53(4)
C2	3.0038(6)	109.74	107.10(1)
C3	3.1478(7)	109.59	106.94(2)
C4	2.633(1)	91.29(5)	88.71(5)

[a]Mean values over the 8 independent units composing the 1D polymeric chain, see ref 12 for all data. [b]Data from the SCXRD structure.

Starting from **A8** (G = H) and **A9** (G = 5-OMe) bearing Me$_2$tn bridge and coordinated primary amino group, the asymmetric unit is composed of one $[Cu(^{G}L3^{H,H})(Cl)]$ independent moiety in both cases, which assembles in dimeric units $[Cu_2(\mu\text{-}Cl)_2(^{H}L3^{H,H})_2]$ with bridging chlorido ions between the two copper(II) ions, as previously observed for **A2**/**A3** and **A5**/**A6** bearing en and tn bridges, respectively, and the coordinated primary amino group.[12,13] Coordination bond distances and angles are listed in Table S4 in Supporting Information.

The coordination environment of each copper(II) ion can be described as square pyramidal with an elongated apical position, where the square plane is formed by the NNO donor set from the $(^{G}L3^{H,H})^{-}$ ligands and by a Cl^{-}. The latter also behaves as a

Downloaded from pubs.acs.org/cgdefu/article-pdf/26/21/9073/6889211/cg6c01323.pdf by UNIV DEGLI STUDI DI MODENA user on 06 November 2026

https://doi.org/10.1021/acs.cgd.6c01323
Cryst. Growth Des. 2026, 26, 9073−9084

Table 3. Intra- and Inter-dimer/chain H-Bond Structural Parameters for the a Series with Coordinated Primary Amino Group[a]

	Intradimer/chain H-bond			Interdimer/chain H-bond					
	N···O (Å)	H···O (Å)	N−H···O (°)	N···Cl (Å)	H···Cl (Å)	N−H···Cl (°)	N···O (Å)	H···O (Å)	N−H···O (°)
A1[a]	3.53	2.75	145	3.32	3.15	95	3.15	2.25	160
A2	3.1106(12)	2.28	152.0	3.386(1)	2.87	117.6	3.697(1)	2.80	168.3
A3	3.229(3)	2.39	152.9	3.426(3)	2.89	119.3	3.051(3)	2.20	154.4
A5	3.069(1)	2.19	162.0	3.662(1)	3.34	103.8	3.361(1)	2.46	169.9
A6	3.193(2)	2.41	147.4	3.488(2)	2.96	119.9	3.445(2)	2.59	162.0
A8	3.039(5)	2.17	158.4	3.312(4)	2.49	150.1	-	-	-
A9	3.088(3)	2.23	160.7	3.321(3)	2.52	150.7	-	-	-

[a]Mean values over the 8 independent units composing the 1D polymeric chain, see ref 12. for all data.

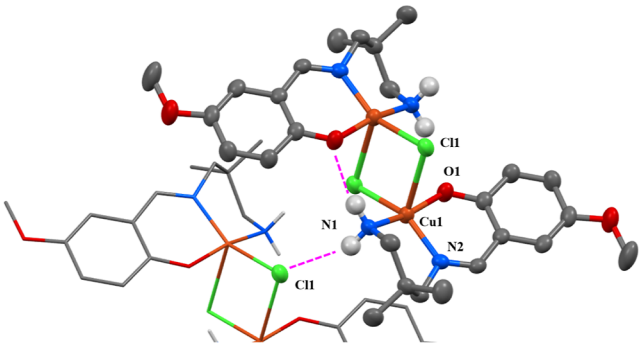

Figure 1. Molecular structure of **A9** with main atom numbering together with intradimer N−H···O and interdimer N−H···Cl H-bonds highlighted as purple dashed lines. Ellipsoids were drawn at the 50% probability level. Color code: Cu = orange, Cl = green, O = red, N = blue, C = grey, H atoms but NH_2 omitted for clarity.

fifth ligand for the adjacent copper(II) ion of the inversion-symmetry-related molecule. The chlorido bridge is asymmetric, with a short Cu−Cl bond in the square, albeit distorted, coordination plane and a longer one as the fifth, almost apical interaction (see Table 2 for structural features). There are also moderately strong intradimer N−H···O H-bonds between the hydrogen of the amino group of one moiety and the phenolic oxygen of the other one to consolidate the dimeric unit (see Table 3 for D···A, H···A, and D−H···A structural parameters).

Dimeric units in **A8** and **A9** are held together by interdimer N−H···Cl H-bonds (see Table 3), giving rise to parallel 1D pillars running along the *a* axis in two different orientations (Figure 1 for **A9** and Figure S2 in Supporting Information for **A8**). Moving to **A2**/**A3** (en) and **A5**/**A6** (tn), whose molecular structures were previously described,[12,13] the absence of steric hindrance of Me_2tn bridge allows the dimeric units to pack differently from **A8**/**A9** and favors both N−H···O and N−H···Cl H-bonds (see Table 3), where the first ones possess a higher degree of linearity (155°−170°) compared to the second ones (95°−120°), and both have a modulated length by the G group and diamine bridge. In all cases, 1D pillars of dimeric units have two different orientations within the crystal packing, but both run parallel to the *a* axis. Surprisingly, in **A3**, interdimer N−H···O bonds are stronger than intradimer ones.

In **A1** (G = 5-NO_2, en), [Cu($^{5-NO2}$L1^{H,H})(Cl)] moieties interact with each other, forming 1D polymeric chains through Cu−Cl···Cu bonds (Table 2). These chains are held together by N−H···O and N−H···Cl H-bonds forming zig−zag 2D layers, packed together in a nested fashion between the alternating nitro groups (see Table 3 and Figure S3 for crystal packing). As for **A3**, **A1** possesses stronger interdimer N−H···O bonds than the intradimer ones. It is then apparent that the substituent has a guiding role in forming interdimeric (G = H) or interpillars/chain (G = OMe, NO_2) H-bonds. Unfortunately, no single crystals or microcrystalline powders could be obtained for **A4** and **A7**, so no comparison can be made with the nitro derivatives with tn and Me_2tn. The presence of the coordinated primary amino group strongly drives the formation of dimeric units via Cl and N−H···O interactions, irrespective of the aliphatic bridge. The only exception is **A1**, where the electron-withdrawing effect of the nitro group prevails and favors 1D chains, which are always stabilized by intrachain N−H···O H-bonds.

For **B1**−**B5**, the asymmetric unit is still composed of [Cu(^{G}Ln^{H,Me})(Cl)] (n = 1, 2) independent moieties, as observed for **A** derivatives. In all cases but **B4**, adjacent units are rotated by 180° and packed into pseudo zig−zag 1D chains through short apical Cu···Cl interactions (see Table 2) together with moderately strong N−H···O H-bonds (**B1**: *d*(H···O1) = 2.26 Å, *d*(N1···O1) = 3.062 Å, angle N1−H···O1 = 152.7°; **B2**: *d*(H···O1) = 2.34 Å, *d*(N1···O1) = 3.134(9) Å, angle N1−H···O1 = 135.9°; **B3-I**: *d*(H···O1) = 2.26 Å, *d*(N1···O1) = 3.132(6) Å, angle N1−H···O1 = 144.6°; and **B5**: *d*(H···O1) = 2.04 Å, *d*(N1···O1) = 2.907 Å, angle N1−H···O1 = 165.54°). The strength of the N−H···O H-bonds is mostly comparable among **B1**−**B3-I**, while it gets stronger in **B5** (shorter and more linear, Figure 2). This is also reflected in the shortest apical Cu···Cl interaction in this last derivative, indicating that the change of the aliphatic bridge from en to tn is not innocent. Indeed, the angles around copper are modulated by the more flexible tn chain, which causes a gradual distortion from square planar with fifth apical interaction toward trigonal bipyramidal (see Table S4 in Supporting Information for full coordination bond distances and angles).

Dimeric assemblies are disfavored due to the presence of only one N−H bond able to act as a H-bond donor, and the overall energetic crystal packing stabilization is reached in chains, which have one (**B3-I**) or two (**B1**, **B2**, and **B5**) orientations running parallel to the shortest crystallographic axis and interact each other through the $\pi\cdots\pi$ stacking of the NO_2-sal moieties (**B1**) or weak van der Waals interactions, i.e., no specific contacts, mainly caused by the aliphatic bridge and the methyl groups (**B2**, **B3-I**, and **B5**).

Interestingly, **B3** can crystallize as dinuclear [Cu_2($^{S-O-Me}$L1^{H,Me})(Cl)]$_2$ (**B3-II**), where 1 chlorido anion and the phenoxido oxygen atom of one tridentate ligand act as bridging units among 2 copper(II) ions. Both copper(II) ions are square pyramidal with a fifth elongated apical position. In particular, Cu1A brings one NNO tridentale ligand and the bridging phenoxido oxygen atom of the adjacent unit in the square plane and the bridging chlorido anion as an apical ligand. Cu2A brings

Downloaded from pubs.acs.org/cgdefu/article-pdf/26/21/9073/6889211/cg6c01323.pdf by UNIV DEGLI STUDI DI MODENA user on 06 November 2026

https://doi.org/10.1021/acs.cgd.6c01323
Cryst. Growth Des. 2026, 26, 9073−9084

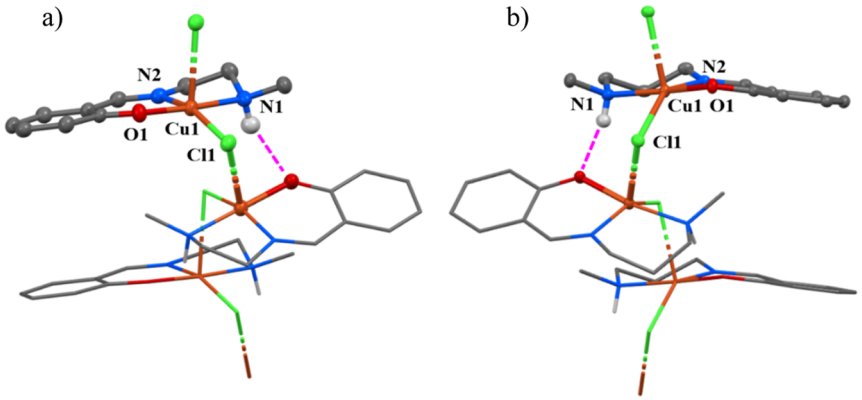

Figure 2. Comparison of crystal packing of (a) **B2** and (b) **B5** with main atom numbering together with short Cu···Cl interactions and intrachain N−H···O H-bonds highlighted as purple dashed lines. Ellipsoids were drawn at the 50% probability level. Color code: Cu = orange, Cl = green, O = red, N = blue, C = grey, H atoms but NH omitted for clarity.

the second NNO tridentale ligand and bridging chlorido anion in the square plane and a second chlorido anion as the fifth apical ligand (see Table S5 in Supporting Information for coordination bond distances and angles). This last is involved in a relatively strong N−H···Cl H-bond with the amino group coordinated to Cu1A (H1A···Cl1B = 2.305 Å, N1A···Cl1B = 3.263(5) Å, and N1A−H1A···Cl1B = 160.3°), which stabilizes the overall dinuclear complex. The hydrogen atom of the amino group coordinated to Cu1B is instead involved in a comparable N−H···Cl H-bond with Cl1B of a second dinuclear unit (H1B···Cl1B = 2.312 Å, N1B···Cl1B = 3.248(6) Å, and N1A−H1A···Cl1B = 155.5°), thus forming a zig-zag 1D chain of dinuclear entities aligned along the *a* axis (see Figure 3 for comparison of **B3-I** and **B3-II**). There are two different orientations of these zigzag chains, which interact through $\pi\cdots\pi$ stacking and weak van der Waals interactions. The crystallization conditions play a role in determining the formation of **B3-I** (slow diffusion of Et_2O into the MeOH reaction mixture) against **B3-II** (slow evaporation of MeOH). The concentration of the species in solution but also the nature of the solvent (only protic and polar versus a more aprotic and less polar when Et_2O is added) probably guides the crystal growth, suggesting a kind of "template effect" even if no solvent molecules are present in the final structures in both cases.[21]

B4 shows an unprecedented polymeric 1D chain where independent [Cu(^{NO2}L2^{H,Me})(Cl)] units are held together via very short Cu−Cl bonds (Table S4) together with a sixth quite short interaction with the phenoxido oxygen atom of an adjacent unit (Cu···O = 2.639 Å). Copper(II) can be then primarily described as pentacoordinated since the two Cu−Cl distances are comparable and then close to trigonal bipyramidal but also hexacoordinated with a distorted octahedral due to the short Cu···O interaction (see Figure 4 and Table S4 in Supporting Information for coordination bond distances and angles). Indeed, the Cu1−O1 and Cu1−N1 bonds are quite elongated (1.9544(4) and 2.0909(4) Å, respectively) compared to other derivatives, and hence, copper(II) eagers more electron density to expand its environment. The cause of the long distance with the phenoxido oxygen atom mainly comes from the electron-withdrawing effect of the nitro group, as we previously observed,[10] but also from the bridging nature of this oxygen atom. The peculiarity of this structure is also highlighted by the mostly negligible effect of the very weak N−H···Cl H-bond (H1···Cl1 = 3.619 Å, N1···Cl1 = 4.552 Å, N1−H1···Cl1 = 146.7°). The 1D chains are stacked only by weak van der Waals interactions, mainly caused by the aliphatic tn bridge and the methyl group.

Moving to derivatives **C1**−**C3** with NMe_2, the asymmetric units in the crystal structure are the [Cu(^{G}L1^{Me,Me})(Cl) moieties in all cases with coordination geometry close to square planar with the NNOCl environment. Even in the absence of possible H-bonds, **C1** is still packed in a pseudo-zig−zag 1D chain composed of stacked units rotated by less than 180° from each other, with the fifth apical position occupied by the chlorido ion of an adjacent unit. The 1D chain runs along the *b* axis (the shortest one). A similar crystal packing can be also observed for **C2** and **C3**, where the pseudo zig−zag 1D chains are composed of stacked units rotated by about 90° from each other and running along the *a* axis, always the shortest crystallographic one (Figure 5).

Going from **C1** to **C3**, there is progressive diminishing of the Cu1−O1 bond length and a gradual elongation of the Cl···Cu apical position, together with a reduction of the Cu−Cl···Cu angle. This angle is close to 90° in the case of **C1**, where the copper(II) eagers more electron density from the apical coordination due to the electron-withdrawing effect of the nitro group (see Table S4 in Supporting Information for coordination bond distances and angles). The pseudo-zig−zag 1D chains are packed through weak C−H···O and C−H···π interactions. Furthermore, the crystal packing of **C1**−**C3** closely resembles that of **B1**−**B3-I**, meaning the role of the en bridge in driving the coordination environment and the assembly of the [Cu(^{G}L1$^{H/Me,Me}$)(Cl)] units. The stabilizing effect of the N−H···O H-bonds is, of course, absent in **C1**−**C3** since this can be present only for **B1**−**B3-I**. Nevertheless, this H-bond seems to influence the fifth Cu···Cl apical position to a greater extent only for **B1**. Indeed, the Cu···Cl distance is longer than in all the other cases with an additional sixth interaction (3.265 and 3.675 Å), while it follows a similar bond length trend in the other cases (2.940(2) and 3.116(2) for **B2**−**B3-I** and 2.7101(11), 3.0038(6), and 3.1478(7) for **C1**−**C3**).

Considering **C4**−**C6**, the effect of the longer bridge and the two methyl groups on the coordinated amine nitrogen atom ($tnMe_2$), in combination with the electronic withdrawing or donating power of the G group, leads to the first dimer assembly [Cu_2(^{NO2}L2^{Me,Me})$_2$(μ-Cl)$_2$] (**C4**) via the Cl bridge in the presence of the nitro group without the stabilization of the intradimer N−H···O H-bonds. The higher basicity of NMe_2

Downloaded from pubs.acs.org/cgdefu/article-pdf/26/21/9073/6889211/0/cg6c01323.pdf by UNIV DEGLI STUDI DI MODENA user on 06 November 2026

https://doi.org/10.1021/acs.cgd.6c01323
Cryst. Growth Des. 2026, 26, 9073−9084

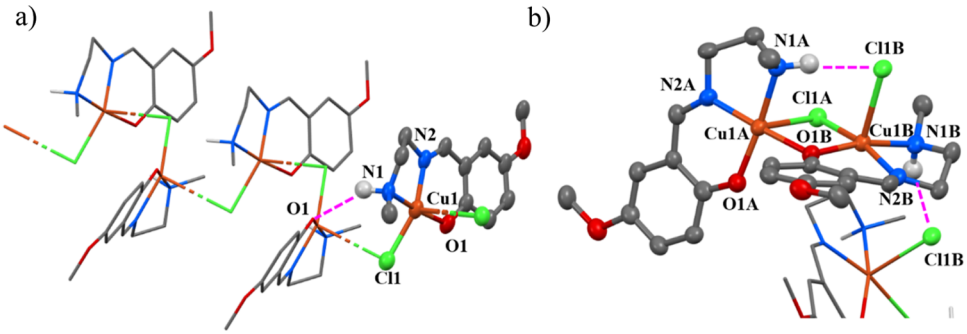

Figure 3. Comparison of (a) **B3-I** and (b) **B3-II** with main atom numbering together with short Cu···Cl interactions and intrachain/dimer N−H···O or N−H···Cl H-bonds highlighted as purple dashed lines. Ellipsoids were drawn at the 50% probability level. Color code: Cu = orange, Cl = green, O = red, N = blue, C = grey, H atoms but NH omitted for clarity.

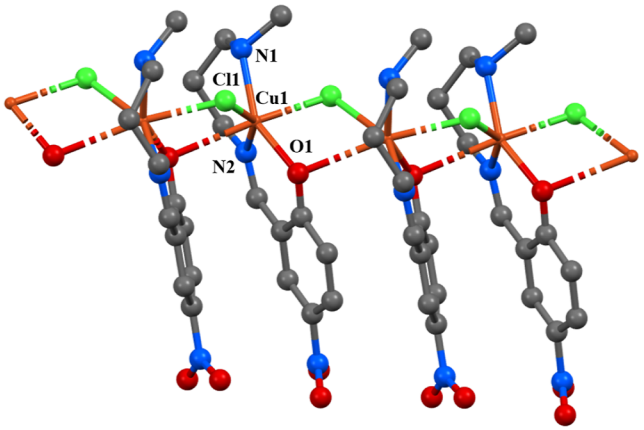

Figure 4. Molecular structure of **B4** with main atom numbering together with short Cu···Cl and Cu···O intrachain interactions. Ellipsoids were drawn at the 50% probability level. Color code: Cu = orange, Cl = green, O = red, N = blue, C = grey, H atoms omitted for clarity.

together with the flexibility of the tn bridge allows the stabilization of such an assembly with an increase of the distortion of the square pyramidal coordination environment, as outlined by the higher displacement of the amine nitrogen atom from the CuNOCl least squares plane (0.96 Å) and concomitant elongation of the Cu1−N1 bond (2.128(4) Å) and shortening of the fifth Cu1···Cl1 distance (2.6324(15) Å). This is also an induced effect of the higher steric hindrance caused by the two methyl groups and the impossibility to create a stabilizing N−H···O H-bond (Figure 6a). In this respect, a comparison with **B4** should be made, where also no N−H···O H-bond was present. The effect of the introduction of the second methyl group on the amino nitrogen atom is then not negligible since it completely changes the crystal packing and hence the coordination of copper(II).

Moving to **C5** and **C6**, the absence of the electron-withdrawing effect of the nitro group makes the phenolato oxygen atom more prone than the chlorido ion to act as a bridging unit between two copper(II) centers. This gives rise to dinuclear assembly $[Cu_2(\mu\text{-}^{G}L2^{Me,Me})_2(Cl)_2]$ (G = H, OMe), where the Cu−O bond distances from one unit to the second metal ion is shorter (about 1.95 Å) than within its belonging unit (about 2.10 Å, see Table S6 in Supporting Information for full coordination bond distances and angles). A similar structure to **C5** with cadmium(II) has been previously reported.[22] The chlorido ions act as the fifth coordination element for both copper(II) ions, and their coordination environment is very close to trigonal bipyramidal (in comparison to the square planar with fifth elongated apical interactions in almost all the other cases, except for **B4**). The axial positions are occupied by the iminic nitrogen and the phenolato oxygen, while the other donors complete the trigonal base (Figure 6b for **C5** and Figure S4 in Supporting Information for **C6**). The higher flexibility given by the tn bridge, together with the impossibility to create stabilizing N−H···O H-bonds, can be sought as driving forces toward the change in the observed dinuclear assembly, since such a solid-state structure is not observed in **C2** and **C3**, where the lower flexibility of the en bridge does not allow to promote a trigonal bipyramidal arrangement with the NMe_2 fragment occupying an equatorial position, as in the case of **C5** and **C6**. $[Cu_2(\mu\text{-}^{G}L2^{Me,Me})_2(Cl)_2]$

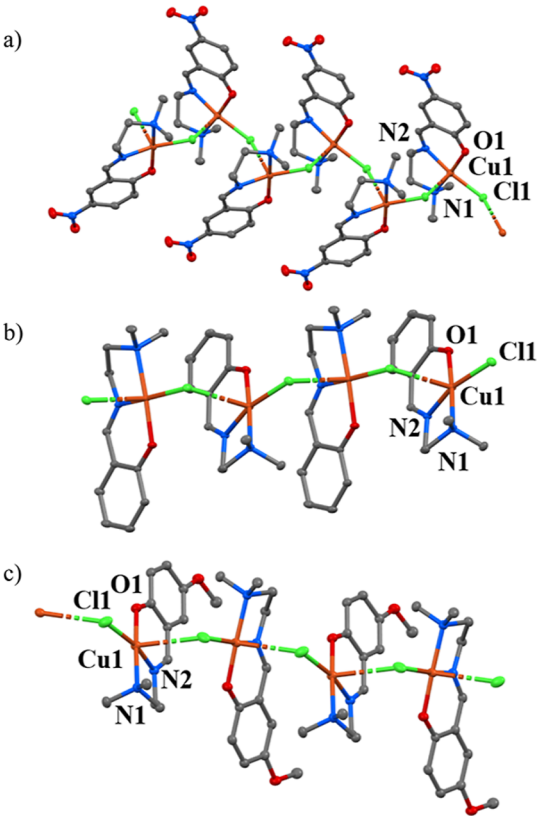

Figure 5. Comparison of the molecular structures of (a) **C1**, (b) **C2**, and (c) **C3** with main atom numbering. Ellipsoids were drawn at the 50% probability level. Color code: Cu = orange, Cl = green, O = red, N = blue, C = grey, H atoms omitted for clarity.

Downloaded from pubs.acs.org/cgdefu/article-pdf/26/21/9073/6889211/0/cg6c01323.pdf by UNIV DEGLI STUDI DI MODENA user on 06 November 2026

https://doi.org/10.1021/acs.cgd.6c01323
Cryst. Growth Des. 2026, 26, 9073−9084

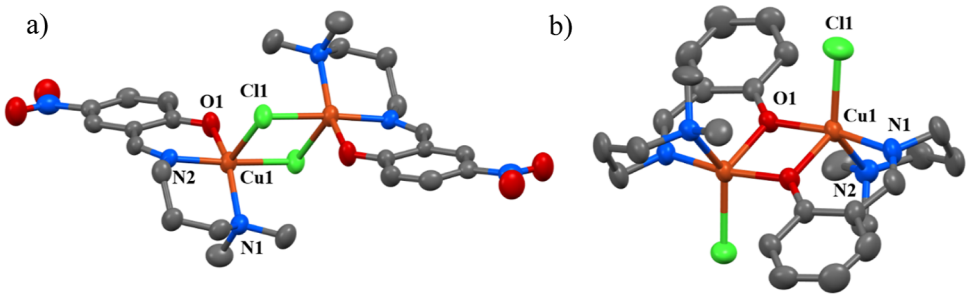

Figure 6. Molecular structure of (a) **C4** and (b) **C5** with main atom numbering. Ellipsoids were drawn at the 50% probability level. Color code: Cu = orange, Cl = green, O = red, N = blue, C = grey, H atoms omitted for clarity.

(G = H, OMe) units are then packed through weak C−H···Cl and van der Waals interactions, giving 1D pillars running along the *a* axis.

General Framework for Crystal Packing

We previously demonstrated that applying a multivariate approach through PCA to structural parameters of iron(II) complexes able to undergo spin crossover (SCO) in the solid state could proficiently map crystal packing effects and help distinguish SCO-active compounds from high-spin-blocked ones.[14] We then decided to apply a similar approach to analyze coordination bonds and angles of our copper(II) complexes. The aim is to disentangle the relative impacts of the steric hindrance of the diamine bridge (L1, L2, and L3), the presence of substituents of the sal moieties (G), and the degree of alkylation of the amino group (R1, R2) in driving the crystal packing. Indeed, all these factors act together in a strict and subtle fashion. In addition, homologous derivatives **P1**−**P22** available in the literature (Table S1 in Supporting Information)[23−37] bearing a NNO tridentate Schiff base ligands derived from G-salH and aliphatic diamines en, tn, and Me_2tn and their alkylated versions on the amino group are included in this study.

Compounds **P10**,[30] **P18**,[34] and **P21**[36] were excluded since they include co-crystallized solvent molecules ($CHCl_3$, H_2O, and MeOH, respectively), which alter the H-bonds among [($^{G}Ln^{R1,R2}$)Cu(Cl)] units. **B4** was also excluded from the PCA model since it possesses a peculiar coordination environment far different from all the other derivatives, with two Cu−Cl bonds and a sixth quite short Cu···O interaction. Data from single crystals were used for **B5**. Indeed, this selection is an essential part of the construction of a sound and robust dataset for chemometric multivariate models. We included only derivatives mainly possessing an NNOCl square planar environment around the copper(II) ion and then extracted their coordination parameters with the following numbering: O1 phenolato oxygen atom, N1 amino nitrogen atom, N2, imino nitrogen atom, and Cl chlorido anion. The four coordination bonds and the six angles represent the 10 variables for 38 complexes from which PCA extracted information by rotating the original space in a constructed space so that each new variable, called a principal component (PC), is orthogonal to the others and that each new variable explains the maximum possible fraction of variance of the data not yet explained by the previous PCs. The PCs are linear combinations of the original variables; the first PC is in the direction of maximum variability of the data, the second is uncorrelated with the first (the two axes are orthogonal) and explains the maximum residual variance fraction, and so on.

PCA, being an unsupervised data analysis tool, allows inspection of the main sources of variability and the "natural" grouping tendencies in the data without imposing any a priori information. A PCA model with two PCs describing 55% of the variance was developed. From the PC1 vs PC2 scores plot with a symbol legend corresponding to the diamine bridge (L1 in red, L2 in green, and L3 in blue) (Figure 7), we can recognize a good grouping based on the steric hindrance imparted by the diamine employed. The L1 derivatives are indeed grouped around the origin of the orthogonal axes, and this is a clear reflection of the higher rigidity of the two-carbon-atom en bridge that imparts a lower degree of variability to the coordination bonds and angles. This appears also in the PC1 vs PC2 loadings plot (Figure S5 in Supporting Information), which shows how the structural parameters influence the position of the complexes in the scores plot. All 10 variables, forming almost a ring around zero, contribute to moving the most flexible derivatives from the origin of the axes, i.e., tn and Me_2tn compounds.

P20 and **P22** show negative PC1 scores, while all other L2 and L3 derivatives have positive PC1 scores. The punctual analysis of these two compounds reveals that **P20** has an OH as the substituent in position 4 on the sal moiety involved in a very strong O−H···O H-bond (O1···O2 = 2.639(4) Å) that drives the crystal packing, while **P22** has the combined presence of naphthalene moieties and the diamine Me_2tnMe_2 forming multiple C−H···π interactions. These intermolecular contacts indeed influence the coordination environment of copper(II), in particular the Cu−N1 bond and N1−Cu−Cl angle, as evidenced by the loadings plot (Figure S5 in Supporting Information). The absence of H-bonds and apical Cu···Cl interactions allows these variables to freely adapt to compensate for the other intermolecular needs. Indeed, if we look at the PC1 vs PC2 scores plot colored according to the degree of alkylation of the amino group (H,H in red, H,R in green, and R,R in blue; R can be any substituent; Figure 8), **P20** and **P22**, showing negative PC2 scores, are far from the grouping of the derivatives with no N−H···O or N−H···Cl H-bonds with positive PC2 scores, confirming the different nature of the intermolecular interactions in these two derivatives. **C4** is also far from the R,R derivatives, and we already noticed its structural peculiarity in forming dimeric units even in the presence of the nitro group, which tends to promote chain assemblies, and in the absence of stabilizing intra-dimeric N−H···O H-bonds. H,H complexes show instead a satisfactory grouping in both PC1 and PC2 positive scores, while H,R derivatives are more scattered, probably due to the mixed substitution. Nevertheless, the allocation of H,R compounds is concentrated in between the H,H and R,R groupings, thus well delimiting the two areas.

The same distinction of compounds able to carry out H-bonds in the crystal packing from the ones with no N−H bonds can be envisaged by considering the PCA model

Downloaded from pubs.acs.org/cgdefu/article-pdf/26/21/9073/6889211 0/cg6c01323.pdf by UNIV DEGLI STUDI DI MODENA user on 06 November 2026

https://doi.org/10.1021/acs.cgd.6c01323
Cryst. Growth Des. 2026, 26, 9073−9084

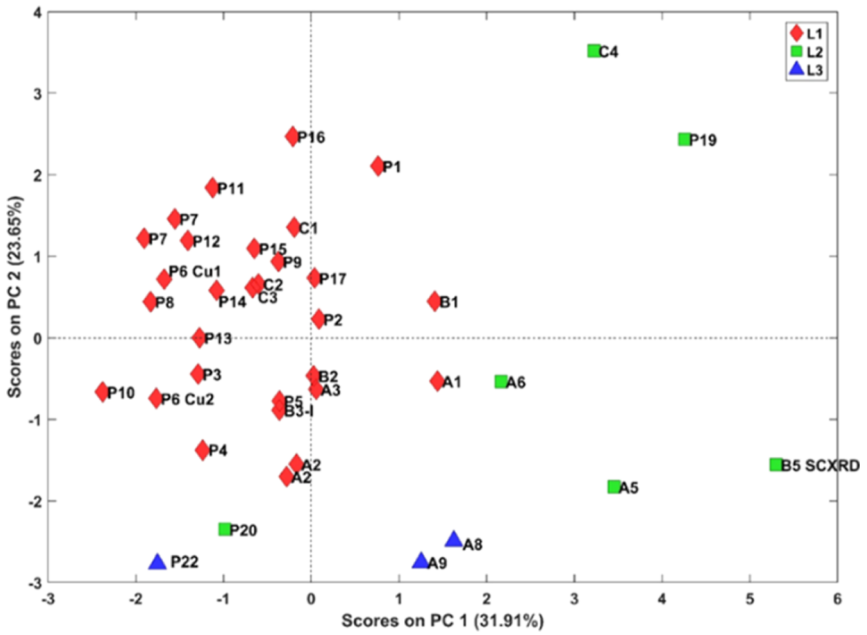

Figure 7. PC1 vs PC2 scores plot for the PCA model constructed including all the 10 variables for the 38 complexes; a symbol legend corresponding to the diamine bridge (L1 in red, L2 in green, and L3 in blue) was applied; labels are added for all complexes.

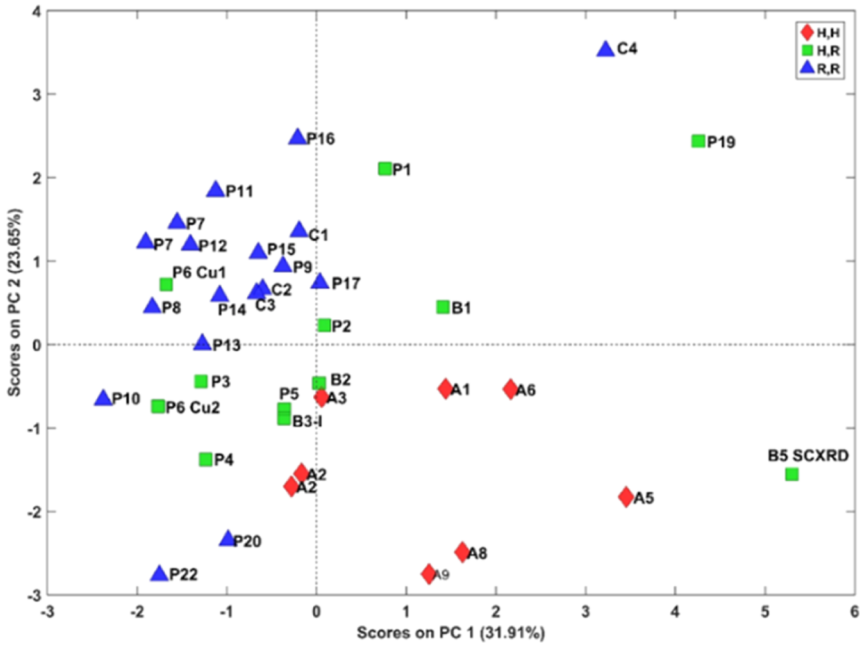

Figure 8. PC1 vs PC2 scores plot for the PCA model constructed including all the 10 variables for the 38 complexes; a symbol legend corresponding to the degree of alkylation of the amino group (H,H in red, H,R in green, and R,R in blue; R can be any substituent) was applied; labels are added for all complexes.

constructed with only the 29 L1 derivatives, where the rigidity of the two-carbon-atom bridge is constant, and all 10 variables. Two principal components were retained, describing 51% of the total variance. The PC1 vs PC2 scores plot colored according to the degree of alkylation of the amino group (H,H in red, H,R in green, R,R in blue; R can be any substituent; Figure 9) clearly shows the grouping of derivatives with completely alkylated amino groups from the others. It is possible to see a trend along the diagonal of the second and fourth quadrant (from negative PC1 and positive PC2 scores to positive PC1 and negative PC2 scores) linked to the degree of alkylation. The two most relevant variables in contributing to this trend are Cu−N1 and N1−Cu−Cl (PC1 vs PC2 loadings plot reported in Figure S6 in Supporting Information). **A1**−**A3** derivatives are also well aligned in the PC1 vs PC2 scores plot and distinguishable from the others.

The synergism among the different steric and electronic factors, together with the presence or absence of H-bonds, can be then efficiently mapped and find its expression in the analysis of copper(II) coordination bonds and angles.

Downloaded from pubs.acs.org/cgdefu/article-pdf/26/21/9073/6889211O/cg6c01323.pdf by UNIV DEGLI STUDI DI MODENA user on 06 November 2026

https://doi.org/10.1021/acs.cgd.6c01323
Cryst. Growth Des. 2026, 26, 9073−9084

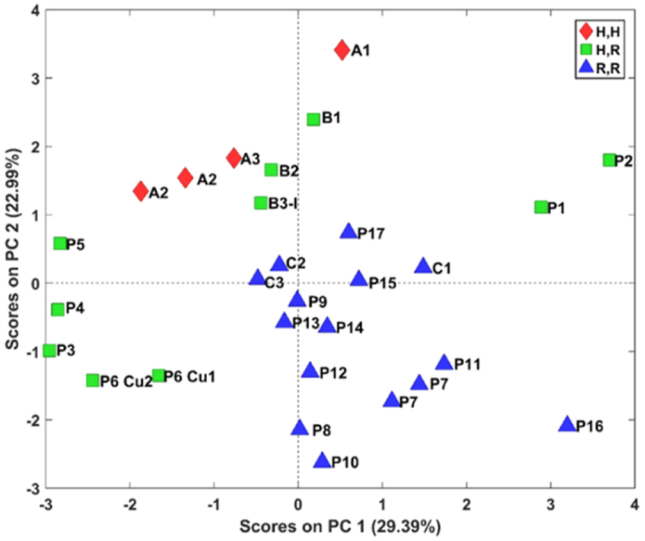

Figure 9. PC1 vs PC2 scores plot for the PCA model constructed including all the 10 variables for the 29 L1 complexes; a symbol legend corresponding to the degree of alkylation of the amino group (H,H in red, H,R in green, and R,R in blue; R can be any substituent) was applied; labels are added for all complexes.

CONCLUSIONS

The extensive synthetic and crystallization efforts devoted to this family of copper(II) complexes bearing NNO tridentate Schiff base ligands and a chlorido ligand revealed remarkable structural diversity. The crystal packing results from a subtle interplay among the electronic character of the substituents, the length and steric hindrance of the diamine bridge, the degree of alkylation of the coordinated amino group, and the ability of the complexes to establish N−H···O and N−H···Cl H-bond interactions. These factors also modulate the coordination environment of copper(II).

Complexes containing a coordinated primary amino group predominantly form dimeric assemblies stabilized by chlorido bridges and N−H···O H-bonds, whereas monoalkylation of the amino group generally promotes pseudo-zig−zag 1D chains. Complete alkylation suppresses N−H···O and N−H···Cl H-bonds, thereby increasing the influence of the flexibility and steric hindrance of the diamine bridge and of the bridging ability of the chlorido or phenoxido oxygen atoms. The observed exceptions and polymorphic behavior further demonstrate that none of these contributions acts independently and that crystallization conditions may also affect the final solid-state assembly.

The multivariate analysis supports these results by revealing grouping tendencies associated with the nature of the diamine bridge and the degree of amino group alkylation. The PCA therefore provides a useful framework for rationalizing how intermolecular interactions are reflected in the copper(II) coordination sphere, and the structural outcome remains governed by the synergistic action of several competing factors.

Looking at the definition of realm in the Cambridge Dictionary, you can find the following: a realm is a country ruled by a king or queen, or a specific area of study, activity, or interest, i.e., it can mean a physical kingdom or an abstract space where an idea or power is dominant. In this sense, the term realm used in the title describes both the structural landscape explored by these compounds and the domain in which sterically and electronically modulated N−H···O and N−H···Cl H-bonds exert their influence. At the same time, this realm is the result of the dedication of many people involved in the synthesis, crystallization, structural characterization, and interpretation of these compounds. If this realm must have a sovereign, it is chemistry itself, which allows us to design, create, and understand the molecular architectures created in the laboratory.

ASSOCIATED CONTENT

Supporting Information

The Supporting Information is available free of charge at https://pubs.acs.org/doi/10.1021/acs.cgd.6c01323.

Experimental section, crystallographic tables for single crystal and powder X-ray diffraction studies, coordination bond distances and angles, molecular structures, and loading plots of PCA analyses (PDF)

Accession Codes

Deposition Numbers 2551458, 2551459, 2551460, 2551461, 2551453, 2551454, 2551456, 2551457, 2560838, 2560839, 2560840, 2560841, 2551397, 2551401, 2551452, 2551462, 2551463, 2551464, and 2551469 contain the supplementary crystallographic data for this paper. These data can be obtained free of charge via the joint Cambridge Crystallographic Data Centre (CCDC) and Fachinformationszentrum Karlsruhe Access Structures service.

AUTHOR INFORMATION

Corresponding Author

Luca Rigamonti − *Dipartimento di Scienze Chimiche e Geologiche, Università degli Studi di Modena e Reggio Emilia, 41125 Modena, Italy;* orcid.org/0000-0002-9875-9765; Email: luca.rigamonti@unimore.it

Authors

Matteo Mari − *Dipartimento di Scienze Chimiche e Geologiche, Università degli Studi di Modena e Reggio Emilia, 41125 Modena, Italy*

Stefano Baratti − *Dipartimento di Scienze Chimiche e Geologiche, Università degli Studi di Modena e Reggio Emilia, 41125 Modena, Italy*

Chiara Canovi − *Dipartimento di Scienze Chimiche e Geologiche, Università degli Studi di Modena e Reggio Emilia, 41125 Modena, Italy; Dipartimento di Ingegneria "Enzo Ferrari", Università degli Studi di Modena e Reggio Emilia, 41125 Modena, Italy*

Anita Ballerini − *Dipartimento di Scienze Chimiche e Geologiche, Università degli Studi di Modena e Reggio Emilia, 41125 Modena, Italy*

Francesco Genua − *Dipartimento di Scienze Chimiche e Geologiche, Università degli Studi di Modena e Reggio Emilia, 41125 Modena, Italy; Dipartimento di Ingegneria "Enzo Ferrari", Università degli Studi di Modena e Reggio Emilia, 41125 Modena, Italy;* orcid.org/0009-0009-0284-8623

Kevin D'Addazio − *Dipartimento di Scienze Chimiche e Geologiche, Università degli Studi di Modena e Reggio Emilia, 41125 Modena, Italy*

Samuele Pellacani − *Dipartimento di Scienze Chimiche e Geologiche, Università degli Studi di Modena e Reggio Emilia, 41125 Modena, Italy*

Downloaded from pubs.acs.org/cgdefu/article-pdf/26/21/9073/6889211/cg6c01323.pdf by UNIV DEGLI STUDI DI MODENA user on 06 November 2026

https://doi.org/10.1021/acs.cgd.6c01323
Cryst. Growth Des. 2026, 26, 9073−9084

Alessio Nicolini − *Dipartimento di Scienze Chimiche e Geologiche, Università degli Studi di Modena e Reggio Emilia, 41125 Modena, Italy;* orcid.org/0000-0002-4742-5458

Lara Gigli − *Elettra Synchrotron Trieste, 34149 Basovizza, Trieste, Italy*

Maurizio Polentarutti − *Elettra Synchrotron Trieste, 34149 Basovizza, Trieste, Italy*

Simone d'Agostino − *Dipartimento di Chimica "Giacomo Ciamician", Università di Bologna, 40129 Bologna, Italy;* orcid.org/0000-0003-3065-5860

Dominga Rogolino − *Dipartimento di Scienze Chimiche, della Vita e della Sostenibilità Ambientale, Università di Parma, 43124 Parma, Italy;* orcid.org/0000-0003-2295-5783

Mauro Carcelli − *Dipartimento di Scienze Chimiche, della Vita e della Sostenibilità Ambientale, Università di Parma, 43124 Parma, Italy;* orcid.org/0000-0001-5888-4556

Complete contact information is available at: https://pubs.acs.org/doi/10.1021/acs.cgd.6c01323

Author Contributions

Conceptualization: D.R. and L.R.; Data curation: M.M. and S.P.; Formal analysis: M.M., S.P., and L.R.; Funding acquisition: L.R., L.G., and D.R.; Investigation: M.M., S.B., C.C., A.B., F.G., K.D., S.P., L.G., M.P., and S.D.; Methodology: M.M., S.P., A.N., M.P., and L.R.; Project administration: L.G. and L.R.; Resources: L.R., L.G., and D.R.; Supervision: L.R. and M.C.; Visualization: M.M., S.B., and S.P.; Writing—original draft: M.M. and L.R.; and Writing—review and editing: A.N., S.D., M.C., and L.R.

Notes

The authors declare no competing financial interest.

■ ACKNOWLEDGMENTS

This research was funded by the Italian Ministero dell'Università e della Ricerca (MUR), by the Dipartimento di Scienze Chimiche e Geologiche of the Università degli Studi di Modena e Reggio Emilia through the Fondo Dipartimentale per la Ricerca year 2024 (FDR2024 linea dottorato), and by Elettra Synchrotron (Trieste, Italy), where the majority of the single-crystal and powder X-ray diffraction studies were conducted at the Light Laboratory XRD1 and at the Materials Characterization by X-ray diffraction (MCX) beamlines, through the approved proposal 20200030 entitled "X-ray diffraction studies on electronically and sterically modulated cytotoxic copper(II) compounds". The authors would like to thank Lorenzo Marchi for his pioneering work with SCO-active iron(II) complexes and his help with the initial design of the PCA analysis of structural data presented in this paper.

■ REFERENCES

(1) Gilli, G.; Gilli, P. *The Nature of the Hydrogen Bond: Outline of a Comprehensive Hydrogen Bond Theory; IUCr Monographs on Crystallography*; Oxford University Press: Oxford, 2009.

(2) Desiraju, G. R. Crystal Engineering: From Molecule to Crystal. *J. Am. Chem. Soc.* **2013**, *135* (27), 9952−9967.

(3) Karas, L. J.; Wu, C.; Das, R.; Wu, J. I. Hydrogen Bond Design Principles. *WIREs Comput. Mol. Sci.* **2020**, *10* (6), e1477.

(4) Alkorta, I.; Rozas, I.; Elguero, J. Non-Conventional Hydrogen Bonds. *Chem. Soc. Rev.* **1998**, *27* (2), 163.

(5) Huang, S.; Cheemarla, V. K. R.; Tiana, D.; Lawrence, S. E. Experimental and Theoretical Investigation of Hydrogen-Bonding Interactions in Cocrystals of Sulfaguanidine. *Cryst. Growth Des.* **2023**, *23* (4), 2306−2320.

(6) Mazzoni, R.; Roncaglia, F.; Rigamonti, L. When the Metal Makes the Difference: Template Syntheses of Tridentate and Tetradentate Salen-Type Schiff Base Ligands and Related Complexes. *Crystals* **2021**, *11* (5), 483.

(7) Rigamonti, L.; Cinti, A.; Forni, A.; Pasini, A.; Piovesana, O. Copper(II) Complexes of Tridentate Schiff Bases of 5-Substituted Salicylaldehydes and Diamines - The Role of the Substituent and the Diamine in the Formation of Mono- Di- and Trinuclear Species - Crystal Structures and Magnetic Properties. *Eur. J. Inorg. Chem.* **2008**, *2008* (23), 3633−3647.

(8) Rigamonti, L.; Forni, A.; Pievo, R.; Reedijk, J.; Pasini, A. Synthesis Crystal Structures and Magnetic Properties of Dinuclear Copper(II) Compounds with NNO Tridentate Schiff Base Ligands and Bridging Aliphatic Diamine and Aromatic Diimine Linkers. *Dalton Trans.* **2011**, *40* (13), 3381−3393.

(9) Rigamonti, L.; Forni, A.; Sironi, M.; Ponti, A.; Ferretti, A. M.; Baschieri, C.; Pasini, A. Experimental and Theoretical Investigations on Magneto-Structural Correlation in Trinuclear Copper(II) Hydroxido Propellers. *Polyhedron* **2018**, *145*, 22−34.

(10) Rigamonti, L.; Demartin, F.; Forni, A.; Righetto, S.; Pasini, A. Copper(II) Complexes of Salen Analogues with Two Differently Substituted (Push−Pull) Salicylaldehyde Moieties. A Study on the Modulation of Electronic Asymmetry and Nonlinear Optical Properties. *Inorg. Chem.* **2006**, *45* (26), 10976−10989.

(11) Rigamonti, L.; Forni, A.; Cariati, E.; Malavasi, G.; Pasini, A. Solid-State Nonlinear Optical Properties of Mononuclear Copper(II) Complexes with Chiral Tridentate and Tetradentate Schiff Base Ligands. *Materials* **2019**, *12* (21), 3595 10.3390/ma12213595.

(12) Rigamonti, L.; Reginato, F.; Ferrari, E.; Pigani, L.; Gigli, L.; Demitri, N.; Kopel, P.; Tesarova, B.; Heger, Z. From Solid State to *in Vitro* Anticancer Activity of Copper(II) Compounds with Electronically-Modulated NNO Schiff Base Ligands. *Dalton Trans.* **2020**, *49*, 14626−14639.

(13) Canovi, C.; Genua, F.; D'Addazio, K.; Gigli, L.; Forni, A.; Michálek, P.; Carcelli, M.; Rogolino, D.; Rigamonti, L. Studies on the Effect of Diamine Elongation in Copper(II) Complexes with NNO Tridentate Schiff Base Ligands. *Inorganics* **2025**, *13* (3), 94.

(14) Marchi, L.; Fantuzzi, S.; Cingolani, A.; Messori, A.; Mazzoni, R.; Zacchini, S.; Cocchi, M.; Rigamonti, L. A Proficient Multivariate Approach for Iron(II) Spin Crossover Behaviour Modelling in the Solid State. *Dalton Trans.* **2023**, *52* (22), 7684−7694.

(15) Piovesana, O.; Chiari, B.; Cinti, A.; Sulpice, A. Synthesis, Structure, and Magnetic Properties of $Cu_2L_2Cl_2$ (LH = *N*-Salicylidene-1,2-Ethanediamine) - A New $S = 1/2$ Spin-Liquid Candidate. *Eur. J. Inorg. Chem.* **2011**, *2011* (28), 4414−4420.

(16) Stoica, A.-C.; Damoc, M.; Cojocaru, C.; Nicolescu, A.; Shova, S.; Dascalu, M.; Cazacu, M. Some Theoretical and Experimental Evidence for Particularities of the Siloxane Bond. *Molecules* **2022**, *27* (23), 8563.

(17) Costes, J.-P.; Chiboub Fellah, F. Z.; Dahan, F.; Duhayon, C. Role of the Kinetic Template Effect in the Syntheses of Non Symmetric Schiff Base Complexes. *Polyhedron* **2013**, *52*, 1065−1072.

(18) Mandal, S. K.; Nag, K. Synthesis of Phenoxo-Bridged Dicopper(II) Complexes of *N*-(2-Aminoalkyl)Salicylaldimines and Their Use in the Formation of Monohalogeno-Complexes and Non-Symmetrical Quadridentate Schiff-Base Complexes. *J. Chem. Soc., Dalton Trans.* **1984**, (12), 2839−2841.

(19) Coelho, A. *TOPAS Academic V5*, 2012.

(20) Altomare, A.; Cuocci, C.; Giacovazzo, C.; Moliterni, A.; Rizzi, R.; Corriero, N.; Falcicchio, A. *EXPO2013*: A Kit of Tools for Phasing Crystal Structures from Powder Data. *J. Appl. Crystallogr.* **2013**, *46* (4), 1231−1235.

(21) Delegkou, M.-I.; Panagiotou, N.; Papatriantafyllopoulou, C.; Tasiopoulos, A.; Papaioannou, D.; Perlepes, S. P.; Nastopoulos, V. Solvatomorphism with Polar Protic/Aprotic and Non-Polar Solvents in a Series of Complexes Derived from the 5-Phenylimidazole/

Downloaded from pubs.acs.org/cgdefu/article-pdf/26/21/9073/6889211 0/cg6c01323.pdf by UNIV DEGLI STUDI DI MODENA user on 06 November 2026

Tetrafluoroborate/Copper(II) Reaction System. *CrystEngComm* **2024**, *26* (26), 3574−3592.
(22) Roy, S.; Harms, K.; Chattopadhyay, S. Formation of Three Photoluminescent Dinuclear Cadmium(II) Complexes with Cd_2O_2 Cores. *Polyhedron* **2015**, *91*, 10−17.
(23) Ye, L.-J.; You, Z. *Catena*-Poly[[{2-[2-(Isopropylamino)Ethyliminomethyl]-4-Nitrophenolato}copper(II)]-μ-Chlorido]. *Acta Crystallogr. E Crystallogr. Commun.* **2007**, *63* (12), m3137.
(24) Kumari, B.; Kundu, S.; Ghosh, K.; Banerjee, M.; Pradhan, S. K.; Islam, S. M.; Brandão, P.; Félix, V.; Das, D. Exploring (Bio)Catalytic Activities of Structurally Characterised Cu(II) and Mn(III) Complexes: Histidine Recognition and Photocatalytic Application of Cu(II) Complex and Derived CuO Nano-Cubes. *Dalton Trans.* **2018**, *47* (39), 14008−14016.
(25) Devonport, J.; Spencer, J.; Kostakis, G. E. Breaking the Symmetry: C_1 -Salans with (N−H) Backbones. *Dalton Trans.* **2021**, *50* (35), 12069−12073.
(26) Xian, D.-M.; You, Z.-L.; Zhang, M.; Hou, P.; Li, X.-H. Dinuclear Schiff-Base Copper(II) Complexes with Various Bridging Groups. *J. Coord. Chem.* **2011**, *64* (18), 3265−3272.
(27) Das, M.; Ghosh, B. N.; Valkonen, A.; Rissanen, K.; Chattopadhyay, S. Copper(II) Complexes with Tridentate N_2O Donor Schiff Base Isomers: Modulation of Molecular and Crystalline Architectures through Supramolecular Interactions. *Polyhedron* **2013**, *60*, 68−77.
(28) Wang, J.; You, Z. Chlorido{2,4-Dichloro-6-[(2-Diethylaminoethylimino)Methyl]Phenolato}copper(II). *Acta Crystallogr. E Struct. Rep. Online* **2007**, *63* (5), m1200−m1201.
(29) Das, M.; Chattopadhyay, S. Designed Synthesis of Copper(II) and Nickel(II) Complexes with a Tridentate N_2O Donor Schiff Base: Modulation of Crystalline Architectures through CH···π and Anion···π Interactions. *J. Mol. Struct.* **2013**, *1051*, 250−258.
(30) Elias, H.; Hilms, E.; Paulus, H. X-Ray Structures and Spectral Properties of 4-Coordinate Copper(II) and Palladium(II) Complexes with a Tridentate ONN-Schiff Base Ligand. *Z. Naturforsch., B:* **1982**, *37* (10), 1266−1273.
(31) Ikmal Hisham, N. A.; Mohd Ali, H.; Ng, S. W. Chlorido{4-Chloro-2-[(2-Morpholinoethyl)Iminomethyl]Phenolato-κ^3 *N*,*N*′,*O*}copper(II). *Acta Crystallogr. E Struct. Rep. Online* **2009**, *65* (8), m870.
(32) Sang, Y.-L.; Lin, X.-S. Synthesis Crystal Structures, and Antibacterial Activities of Two Copper(II) Complexes Derived from 1-[(2-Morpholin-4-Ylethylimino)Methyl]-Naphthalen-2-Ol. *Transit. Met. Chem.* **2009**, *34* (8), 931−936.
(33) Lei, Y.; Yang, Q.; Hu, Z.; Wang, S. Synthesis, Structural Studies and Antimicrobial Activity of Copper(II) Complexes Derived from 2,4-Difluoro-6-(((2-(Pyrrolidin-1-Yl)Ethyl)Imino)Methyl)Phenol. *Polyhedron* **2024**, *259*, 117071.
(34) Yu, J. A Novel 1D Copper(II) Complex Derived From 2-Bromo-4-Chloro-6-[(2-Morpholin-4-Ylethylimino)Methyl]Phenol: Synthesis and Crystal Structure. *Synth. React. Inorg. Metal-Org. Nano-Metal Chem.* **2014**, *44* (3), 348−351.
(35) Jayendran, M.; Begum, P. M. S.; Kurup, M. R. P. Structural Spectral and Biological Investigations on Cu(II) and Zn(II) Complexes Derived from NNO Donor Tridentate Schiff Base: Crystal Structure of a 1D Cu(II) Coordination Polymer. *J. Mol. Struct.* **2020**, *1206*, 127682.
(36) Ikmal Hisham, N. A.; Khaledi, H.; Mohd Ali, H.; Hadi, H. A. Coordination Modes of Two Flexidentate Salicylaldimine Ligands Derived from *N* -(3-Aminopropyl)Morpholine toward Zinc and Copper. *J. Coord. Chem.* **2012**, *65* (17), 2992−3006.
(37) Kumar Kundu, B.; Chhabra, V.; Malviya, N.; Ganguly, R.; Mishra, G. S.; Mukhopadhyay, S. Zeolite Encapsulated Host-Guest Cu(II) Schiff Base Complexes: Superior Activity towards Oxidation Reactions over Homogenous Catalytic Systems. *Micropor. Mesopor. Mat.* **2018**, *271*, 100−117.

Downloaded from pubs.acs.org/cgdefu/article-pdf/26/21/9073/6889211O/cg6c01323.pdf by UNIV DEGLI STUDI DI MODENA user on 06 November 2026

https://doi.org/10.1021/acs.cgd.6c01323
Cryst. Growth Des. 2026, 26, 9073−9084